

The high-resolution visible overtone spectrum of acetylene^{a)}

George J. Scherer,^{b)} Kevin K. Lehmann, and William Klemperer

Department of Chemistry, Harvard University, Cambridge, Massachusetts 02138

(Received 15 October 1982; accepted 17 December 1982)

Direct, gas-phase overtone spectra of states corresponding to five and six quanta of C–H stretch have been obtained for four isotopically substituted acetylenes in the region 14 900–18 500 cm^{-1} . Peak positions of individual rotation–vibration lines were determined to a precision of about 0.003 cm^{-1} . A total of 39 bands are analyzed: 16 for $^{12}\text{C}_2\text{H}_2$; 14 for $^{13}\text{C}_2\text{H}_2$; five for $^{12}\text{C}^{13}\text{CH}_2$; and four for $^{12}\text{C}_2\text{HD}$. The rotational structure of the bands is fit to a semirigid rotor Hamiltonian. However, the bands suffer from severe rotational perturbations, with typical matrix elements being on the order of 0.3 cm^{-1} or less. The error in the determined band origins varies between 0.001 and 0.1 cm^{-1} , depending on the degree of perturbation. Precision rotational constants are also determined for the observed bands. The vibrational term values cannot be adequately explained in terms of the usual slightly anharmonic normal mode expansion. Even though acetylene represents an intermediate case between the local mode and normal mode limits, the simple local mode theory described by Child and Lawton [M. S. Child and R. T. Lawton, *Faraday Discuss.* **71**, 273 (1981)] can be used to rationalize many aspects of the spectrum—e.g., the splitting of the states $|005^*01^1\rangle$ and $|005^*01^1\rangle$ is found to be only 0.44 cm^{-1} . The intermediate character of acetylene is seen upon single deuterium substitution. The state corresponding to five quanta of ^{12}C –H stretch shifts about 100 cm^{-1} to the blue, a result which is certainly anomalous from the point of view of intuitive local mode theory. The band origins for the observed Σ – Σ transitions for all four acetylenes studied are found to be in good agreement with the results of a recent variational calculation [L. Halonen, M.S. Child, and S. Carter, *Mol. Phys.* **47**, 1097 (1982)]. It is also observed that the anharmonic shifts of the sequence band transitions are quite large—for the $\nu = 5$ overtone band, the sequence bands are shifted 74 cm^{-1} to the Π_g bend and 39 cm^{-1} for the Π_u bend.

I. INTRODUCTION

In recent years, C–H stretching overtone spectra of polyatomic molecules have excited considerable interest. An understanding of these highly vibrationally excited states should be relevant to many areas, such as RRKM theory, infrared multiphoton absorption processes, intersystem crossing, intramolecular vibrational energy transfer, and to “state selective” chemistry. Much of the early work on vibrational overtones was done in the photographic infrared.¹ The more recent spectroscopic investigations of these highly forbidden transitions have been made possible by the development of the tunable dye laser, together with sensitive detection techniques, such as photoacoustic spectroscopy² and thermal lensing.³

Most of the work in this field to date has been done at low resolution and on relatively large molecules, such as benzene.⁴ One consequence of this work has been the development of the “local mode” picture of these highly excited states.⁵ This interpretation of the spectra is supported by the observation of linear Birge–Sponer plots, and by the fact that relatively few bands are observed, compared to the large number anticipated on the basis of the usual normal mode analysis. A second conclusion of this work has been that the initially excited C–H stretching mode undergoes rapid, irreversible, intramolecular vibrational relaxation, giving rise to very broad (about 100 cm^{-1}) featureless, Lorentzian line shapes.^{6,7} Interpretation of the spectra of these large molecules is complicated by several factors. Although the line shapes are suggestive of homogeneous broadening, the features are often only superficially Lorentzian.⁸ Secondly, because these are linear ab-

sorption experiments on a static gas sample, they are incapable of unambiguously distinguishing between homogeneous and inhomogeneous contributions to the line shape. It is not surprising that the overtones of benzene, for example, show no resolvable structure—even the fundamentals of benzene are incompletely resolved in Doppler-limited spectra.⁹

High resolution, rotationally resolved spectra of small polyatomic molecules (e.g., HCN, acetylene) do not suffer from these ambiguities. Even though these smaller systems are less interesting chemically, and are not expected to undergo intramolecular vibrational relaxation, they have the advantage of being much more theoretically tractable. Furthermore, the same interactions that are thought to give rise to local mode behavior and intramolecular vibrational relaxation in large molecules are also present in smaller systems, and hopefully may be quantified therein. Thus, a detailed understanding of highly excited vibrational states and their interactions in small molecules should lead to improved models for the vibrational overtones of larger systems.

To obtain detailed spectroscopic information on the overtones of small polyatomic molecules, we have constructed an automated photoacoustic spectrometer, operating in the visible wavelength region of the spectrum, which is able to give Doppler-limited resolution. Our results on the simplest of polyatomic monohydrides, HCN, and its isotopically substituted analogs, have already been reported.¹⁰ The present paper reports our work on the somewhat more complicated molecule acetylene.

II. THEORY

Despite the fact that Mecke introduced a bond mode description of the overtones of acetylene in the 1930's,¹¹ the modern interest in the local mode model for the description of vibrations in polyatomic molecules is a relatively recent development, compared to the traditional normal mode treatment. It is therefore not surprising that neither the nomenclature¹² nor the interpretation¹³ of the local mode model is standardized. Despite the fact that the local mode picture has been discussed by many authors, it is useful for us to give a brief description of local mode theory here to clarify the definitions and ideas which are used below to describe the spectrum of acetylene.

If the bending coordinates are neglected, the zero order vibrational Hamiltonian for (linear) acetylene is taken to be:

$$H^0 = \sum_{i=1}^3 H_i^0, \quad (1)$$

$$H_i^0 = G_{ii} P_i^2 + V_i(r_i),$$

where r_i denotes the displacement coordinate for the i th oscillator; p_i denotes the conjugate momentum for the i th oscillator; G_{ii} denotes the i th diagonal element of the Wilson G matrix¹⁴; and V_i is the potential for stretching the i th bond. The subscript "1" refers to one C-H stretching coordinate, "2" refers to the C-C stretch, and "3" refers to the other C-H stretch. The zero order functions are then

$$|v_1, v_2, v_3\rangle = |v_1\rangle |v_2\rangle |v_3\rangle,$$

where $|v_i\rangle$ is the v_i th eigenfunction of H_i^0 . This approach differs from the usual normal mode treatment, since in the normal mode basis the G matrix is diagonal at equilibrium, and the bond potentials are taken to be harmonic. Of course, for symmetric acetylenes, one must construct linear combinations of g and u symmetry from these local mode basis functions. However, one of the attractions of the local mode picture is that, for highly excited states in which coupling between local modes can be neglected, the symmetrized and unsymmetrized basis functions should give the same expectation value for any reasonable operator.⁵

The zero order Hamiltonian described above neglects off-diagonal kinetic and potential terms. This will be a good approximation when the off-diagonal couplings are small in magnitude compared to the zero-order energy splittings. The manifold of vibrational states characterized by given values of $v = v_1 + v_3$ and v_2 are nearly degenerate, being split in zero order only by the anharmonicity in $V_i(r_i)$. The most important parts of the Hamiltonian which are neglected in H^0 are those which couple the two C-H oscillators. Neglect of these terms would seem to be a good approximation for the highly excited states of acetylene since there is no direct G -matrix coupling between the two C-H groups. The only kinetic coupling possible is indirect, through the C-C bond. For acetylene, the off-diagonal potential constants are indeed much smaller than the diagonal terms. In the anharmonic force field for C_2H_2 of Strey and Mills the diagonal C-H force constant is $6.37 \text{ aJ}\text{\AA}^{-2}$, while

the off-diagonal force constant between the two C-H groups is $-0.019 \text{ aJ}\text{\AA}^{-2}$.¹⁵

This very simple model Eq. (1) has a number of qualitative predictions for the spectrum of acetylene. First, one would expect the pure C-H stretching overtones to give a linear Birge-Sponer plot.⁵ Second, the isotope shifts are expected to be quite simple.⁶ In $^{12}C^{13}CH_2$ and $^{12}C_2HD$, for example, the band origins for the ^{12}C -H stretching overtones should only be slightly shifted from their frequencies for $^{12}C_2H_2$. The local mode picture, in the simple form so far presented, includes no zero-order interaction between the two ends of the acetylene molecule. Finally, the local mode model allows us to make qualitative predictions of relative intensities.¹² The intensity of overtone transitions involves a complicated interaction between both mechanical and electrical anharmonicity. The intensity for a vibrational transition is given by matrix elements of the dipole moment operator. In the traditional normal mode approximation, the dipole moment operator is expanded in a Taylor series in normal coordinates, which is then truncated at first order:

$$\mu(q_1, q_2, q_3) = \mu_0 + \sum_{i=1}^3 \left(\frac{\partial \mu}{\partial q_i} \right) q_i,$$

where q_i is the displacement coordinate for the i th normal mode. In the local mode picture, the dipole moment is expanded in a similar way, but in terms of bond displacement coordinates

$$\mu(r_1, r_2, r_3) = \mu_0 + \sum_{i=1}^3 \left(\frac{\partial \mu}{\partial r_i} \right) r_i.$$

In this approximation, the strongest bands in the spectrum are expected to be transitions to pure local mode states, e.g., $|00v_i\rangle$. The intensities of these bands are then interpreted as being due to mechanical anharmonicity, i.e., the anharmonicity of the bond potentials $V_i(r_i)$. In a local mode basis, matrix elements of the type

$$\langle v_1, v_2, v_3 | r_1 | 000 \rangle = \langle v_1 | r_1 | 0 \rangle \langle v_2 | 0 \rangle \langle v_3 | 0 \rangle$$

vanish, as long as v_2 and v_3 are not both zero, so intercombination bands will have zero intensity. The intensity that in fact they do have can then be viewed as a measure of the mixing of local mode basis states, with combination bands borrowing intensity from the pure local mode states, e.g., $|00v_i\rangle$. This model readily explains the observation that the relative intensities are

$$|006\rangle > |105\rangle \approx |015\rangle > |204\rangle \approx |024\rangle.$$

If electrical anharmonicity is recognized as being very important to overtone intensities, then intensities cannot be predicted unless a model is chosen for the dipole moment function. If a "bond dipole" approximation is appropriate, the dipole moment operator can be written as

$$\mu(r_1, r_2, r_3) = \mu_1(r_1) + \mu_2(r_2) + \mu_3(r_3).$$

Now the states $|00v\rangle$ get intensity by both mechanical and electrical anharmonicity. Then, as before, a local mode basis set has

$$\langle v_1, v_2, v_3 | \mu | 000 \rangle = 0$$

for no two of v_1 , v_2 , and v_3 both zero. Thus combination bands are still predicted to be weak, getting intensity from local-mode basis state mixing, or from the neglected terms in the dipole moment function that depend upon two or more bond coordinates simultaneously. Previous workers have usually assumed that electrical anharmonicity does not affect the intensity of combination bands, and therefore used the combination band intensity as a quantitative measure of the degree of local mode mixing. However, this appears to have been done more out of a lack of any reliable estimate of the dipole moment function for polyatomic molecules, rather than from a knowledge that the approximations are in fact justified.¹²

To label the observed states of acetylene, we will use a notation in which local mode quantum numbers describe the stretching part of the wave function, and normal mode quantum numbers specify the degree of bending excitation. For $^{12}\text{C}_2\text{H}_2$ and $^{13}\text{C}_2\text{H}_2$, the states are labeled $|v_1, v_2, v_3^{g/u}, v_4^l, v_5^l\rangle$, where v_1 and v_3 denote the local C-H stretches, with the convention that $v_3 > v_1$; g and u denote the symmetry of the linear combination of local C-H stretching basis functions; v_2 is the C-C stretching quantum number; v_4 and v_5 are quantum numbers for the Π_g and Π_u bends, respectively; and l_4 and l_5 are the vibrational angular momentum quantum numbers for the appropriate bending modes. For the unsymmetrical acetylenes $^{12}\text{C}_2\text{HD}$ and $^{12}\text{C}^{13}\text{CH}_2$, the states will be labeled $|v_1, v_2, v_3, v_4^l, v_5^l\rangle$, where v_1 is the quantum number for the ^{12}C -D or ^{13}C -H stretch; v_2 again refers to the C-C stretch; v_3 refers to the ^{12}C -H stretch; and v_4 and v_5 and l are the normal mode bending quantum numbers, as described by Herzberg.¹⁶ For conciseness of notation, the vibrational angular momentum quantum numbers will be suppressed whenever they vanish. The problem of labeling these states is a difficult one. We have chosen our labels so as to be as consistent as possible with the notation of Herzberg.¹⁶

III. EXPERIMENTAL

The details of our experiment have been described previously.¹⁰ Briefly, the detector is a longitudinally resonant photoacoustic cell,¹⁷ placed inside the cavity of a standing wave, cw dye laser, pumped by a visible argon ion laser. The dye laser is frequency modulated at the resonant frequency of the acoustic cell with a modulation depth of 1 GHz; the microphone signal is detected with a lock-in amplifier, giving derivative line shapes. A minicomputer scans the frequency of the dye laser, and simultaneously stores three data channels from independent A/D converters: (1) the photoacoustic signal, (2) interference fringes of a 2 GHz Cervit-spaced Fabry-Perot interferometer, with a finesse of about 4, and (3) an iodine fluorescence signal. The Fabry-Perot fringes are used for scan linearization. The iodine spectrum serves as an absolute frequency reference.¹⁸

All spectra were taken with pressures of between 15 and 25 Torr of sample in the photoacoustic cell. The pressure broadening coefficient for acetylene has been measured to be about 10 MHz (0.0003 cm^{-1}) per Torr for one overtone band,¹⁹ so at these pressures, pres-

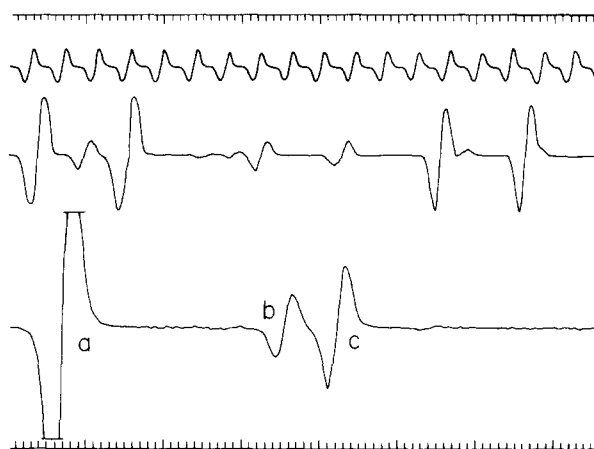


FIG. 1. Spectrum of $^{12}\text{C}_2\text{H}_2$ near 15487 cm^{-1} . Shown top to bottom: etalon transmission peaks 0.07 cm^{-1} apart; I_2 fluorescence; photoacoustic spectrum of acetylene. The three features in the photoacoustic spectrum are: (a) the line P(14) at 15487.406 cm^{-1} of a Π - Π band; (b) the P(14) line at 15487.856 cm^{-1} of a Σ - Σ band of $^{13}\text{C}^{12}\text{CH}_2$ observed in natural abundance; and (c) the P(33) line at 15487.966 cm^{-1} from a Σ - Σ band. This figure has been enhanced by the draftsman for clarity. The noise level in this spectrum is about equal to the pen width ($1/256$ th of full scale).

sure broadening should be almost an order of magnitude less than the Doppler width (about 0.045 cm^{-1}). A sample spectrum of $^{12}\text{C}_2\text{H}_2$ is shown in Fig. 1. The width of the etalon fringes reflects the modulation depth of the laser, not the finesse of the etalon. The high sensitivity of our detector is demonstrated by the high signal to noise displayed in this spectrum. The off-scale line is from a Π - Π hot band. The second line labeled P(14) is from a Σ - Σ band of $^{12}\text{C}^{13}\text{CH}_2$, observed in natural abundance. The resolution of our spectrometer is Doppler limited. We are able to assign peak frequencies for resolved rotational lines to 0.001 cm^{-1} relative precision. The absolute frequency accuracy is about 0.003 cm^{-1} .

The sample of $^{12}\text{C}_2\text{H}_2$ was obtained commercially from Matheson. The spectra of $^{12}\text{C}^{13}\text{CH}_2$ and $^{13}\text{C}_2\text{H}_2$ were observed in an isotopically mixed sample of 90 atom % ^{13}C acetylene, purchased from Merck. The $^{12}\text{C}_2\text{HD}$ was synthesized according to the procedure of Lompa-Krzymien and Leitch.²⁰

IV. RESULTS

A. Σ - Σ bands

Angular momentum quantum numbers were assigned to resolved rotation-vibration lines mostly by inspection. Loomis-Wood plots²¹ were found to be helpful in some cases, especially in the assignment of congested spectra from the isotopically mixed $^{13}\text{C}_2\text{H}_2$ sample. Then ground state combination differences were generated from each band and fit to the usual formula.²² In most cases, these ground state fits gave a standard deviation of 0.003 cm^{-1} or less, and reproduced the known spectroscopic constants to within the error of the fit. This practice gave us a check on the internal consistency and quality of our data. It also acted as a check

TABLE I. Rotational constants of isotopically substituted acetylenes.

State ^a	ν_0 (cm ⁻¹)	B'' (cm ⁻¹)	D'' (cm ⁻¹) $\times 10^6$
		¹² C ₂ H ₂ ^{b,c}	
(0000 ⁰ ₀)	...	1.176 608(14)	1.598(9)
(0001 ¹ ₀)	611.694(2)	1.175 274(21)	1.606(16)
		1.180 507(21)	1.656(16)
(0000 ⁰ ₁)	729.155(2)	1.176 400(18)	1.606(10)
		1.181 090(19)	1.635(11)
		¹³ C ₂ H ₂ ^d	
(0000 ⁰ ₀)	...	1.119 49(4)	1.47(2)
		¹² C ¹³ CH ₂ ^d	
(0000 ⁰ ₀)	...	1.148 40(2)	1.56(2)
		¹² C ₂ HD ^b	
(0000 ⁰ ₀)	...	0.991 527 3(16)	1.120(13)

^aThe states are identified by the normal mode quantum numbers as described in Ref. 16.

^bFrom Ref. 23.

^cFrom Ref. 24.

^dFrom Ref. 25.

on the assignment of a band to a particular isotopic species. As will be discussed later, most of the excited vibrational states we observed were rotationally perturbed at least twice. Consequently, the ground state fits were necessary to distinguish between real perturbations and experimental artifacts. It should be mentioned that the spectra were quite dense, with many blended lines. Many weak features were not assigned.

After ground state combination differences had been fit successfully, the upper state constants were determined from a whole band fit in which the ground state constants were constrained to their literature values²³⁻²⁵ (see Table I). The lines were fit to the polynomial²⁶:

$$\nu(m) = \nu_0 + (2B'' + \Delta B)m + (\Delta B - \Delta D)m^2 - 2(2D'' + \Delta D)m^3 - \Delta Dm^4, \quad (2)$$

where ν_0 is the band origin; m is $-J$ for P -branch lines, $J+1$ for R -branch lines; B'' is the ground state rotational constant; D'' is the ground state distortion constant; ΔB is the difference between the excited state and

TABLE II. Observed and calculated transition frequencies for the Σ - Σ band of ¹²C₂H₂ at 15 600 cm⁻¹.^{a,b,c}

J	$P(J)$ observed	$P(J)$ calculated	O-C	$R(J)$ observed	$R(J)$ calculated	O-C
0		15 602.4521	15 602.4515	0.54
1	15 597.8110	15 597.8110	-0.05	15 604.6725	15 604.6728	-0.29
2	15 595.3932	15 595.3919	1.15	15 606.8286	15 606.8281	0.46
3	15 592.9080	15 592.9070	0.90	15 608.9178	15 608.9173	0.42
4	15 590.3556	15 590.3562	-0.64	15 610.9429	15 610.9405	2.24
5	15 587.7389	15 587.7397	-0.81	15 612.8988	15 612.8975	1.15
6	15 585.0576	15 585.0575	0.09	15 614.7873	15 614.7884	-1.12
7	15 582.3095	15 582.3095	-0.04	15 616.6140	15 616.6132	0.73
8	15 579.4959	15 579.4959	-0.05	15 618.3739	15 618.3717	2.04
9	15 576.6165	15 576.6167	-0.23	15 620.0642	15 620.0640	0.18
10	15 573.6701	15 573.6719	-1.78	15 621.6893	15 621.6899	-0.65
11	15 570.6599	15 570.6617	-1.70	15 623.2502	15 623.2496	0.49
12	15 567.5855	15 567.5859	-0.42	15 624.7428	15 624.7430	-0.20
13	15 564.4437	15 564.4447	-1.00	15 626.1699	15 626.1699	-0.07
14	15 561.2383	15 561.2382	0.09	15 627.5305	15 627.5305	-0.04
15	15 557.9654	15 557.9663	-0.84	15 628.8247	15 628.8246	0.00
16	15 554.6274	15 554.6291	-1.60	15 630.0524	15 630.0523	0.02
17	15 551.2264	15 551.2266	-0.26	15 631.2141	15 631.2135	0.49
18	15 547.7585	15 547.7590	-0.52	15 632.3098	15 632.3082	1.45
19	15 544.2252	15 544.2262	-1.03	15 633.3371	15 633.3364	0.65
20	15 540.6267	15 540.6284	-1.63	15 634.2978	15 634.2980	-0.18
21	15 536.9638	15 536.9655	-1.64	15 635.1913	15 635.1930	-1.60
22	15 533.2371	15 533.2376	-0.52	15 636.0247	15 636.0213	3.12
23	15 529.4456	15 529.4448	0.72	15 636.7841	15 636.7831	0.90
24	15 525.5873	15 525.5871	0.17	15 637.4788	15 637.4782	0.53
25	15 521.6656	15 521.6645	0.96	15 638.1062	15 638.1066	-0.41
26	15 517.6771	15 517.6772	-0.14	15 638.6693	15 638.6683	0.89
27	15 513.6253	15 513.6252	0.09	15 639.1642	15 639.1633	0.81
28	15 509.5082	15 509.5084	-0.26	15 639.5923	15 639.5915	0.67
29	15 505.3276	15 505.3271	0.42	15 639.9529	15 639.9530	-0.15
30		15 640.2465	15 640.2477	-1.18
31		15 640.4746	15 640.4756	-0.99

^aTransition frequencies are in cm⁻¹.

^bResiduals are in units of $\sigma = 0.001$ cm⁻¹.

^cTransitions marked by an asterisk were given zero weight in the fit.

TABLE III. Observed and calculated transition frequencies for the $\Sigma-\Sigma$ band of $^{12}\text{C}_2\text{H}_2$ at $18\,430\text{ cm}^{-1}$.^{a,b,c}

J	$P(J)$ observed	$P(J)$ calculated	O-C	$R(J)$ observed	$R(J)$ calculated	O-C
0		18 432.3347	18 432.3384	-0.91
1	18 427.7125	18 427.7128	-0.08	18 434.5314	18 434.5298	0.37
2	18 425.2796	18 425.2788	0.18	18 436.6406	18 436.6404	0.03
3	18 422.7654	18 422.7641	0.32	18 438.6722	18 438.6701	0.51
4	18 420.1698	18 420.1686	0.28	18 440.6189	18 440.6188	0.02
5	18 417.4921	18 417.4925	-0.10	18 442.4886	18 442.4865	0.50
6	18 414.7361	18 414.7358	0.07	18 444.2785	18 444.2733	1.26
7	18 411.8991	18 411.8985	0.13	18 446.0043*	18 445.9792	6.19
8	18 408.9843	18 408.9808	0.85	18 447.5983	18 447.6040	-1.41
9	18 406.0075*	18 405.9827	6.11	18 449.1467	18 449.1479	-0.30
10	18 402.8987	18 402.9043	-1.38	18 450.6106	18 450.6109	-0.07
11	18 399.7430	18 399.7456	-0.65	18 451.9921	18 451.9929	-0.20
12	18 396.5040	18 396.5068	-0.70	18 453.2944	18 453.2940	0.08
13	18 393.1847	18 393.1880	-0.81	18 454.5179	18 454.5143	0.89
14	18 389.7856	18 389.7892	-0.89	18 455.6584	18 455.6536	1.16
15	18 386.3099	18 386.3106	-0.17	18 456.7138	18 456.7122	0.38
16	18 382.7510	18 382.7522	-0.30	18 457.6939	18 457.6900	0.94
17	18 379.1113	18 379.1142	-0.72	18 458.5919	18 458.5871	1.16
18	18 375.3948	18 375.3967	-0.48	18 459.4128	18 459.4036	5.27
19	18 371.6002	18 371.5999	0.07	18 460.1604*	18 460.1394	5.17
20	18 367.7293	18 367.7237	1.36	18 460.7732*	18 460.7947	-5.30
21	18 363.7818*	18 363.7685	3.26	18 461.3610	18 461.3695	-2.09
22	18 359.7058*	18 359.7343	-7.04	18 461.8661	18 461.8638	0.55
23	18 355.6092	18 355.6213	-2.98	18 462.2810	18 462.2779	0.75
24	18 462.6085	18 462.6117	-0.79
25	18 462.8698	18 462.8654	1.08

^aTransition frequencies are in units of cm^{-1} .^bResiduals are in units of $\sigma = 0.004\text{ cm}^{-1}$.^cTransitions marked with an asterisk were given zero weight in the fit.

ground state rotational constants; and ΔD is the difference between the excited state and ground state rotational constants. Upper state constants were determined from a constrained whole band least-squares fit, rather than from upper state combination differences, because the whole band fit permitted all the observed lines to be included. In most bands, it was necessary to delete several lines in order to obtain a fit with a satisfactory standard deviation. Some of the deleted lines showed evidence of being blended, and others showed clear evidence of upper state perturbations. It should be noted that we have assigned peak frequencies of lines to a relative precision of 0.001 cm^{-1} , which is about $1/40$ of the linewidth. This is made possible by the high signal-to-noise ratio on most lines. However, because we are able to assign peak frequencies so precisely, shifts in the peak frequency due to partially resolved rotational lines represent a severe problem. Ground state combination differences easily distinguish such shifts from perturbations since blending from overlapping bands generally does not affect R and P branch lines in precisely the same way.

The complete results of fits for two $\Sigma-\Sigma$ bands of $^{12}\text{C}_2\text{H}_2$ are given in Tables II and III. Table II shows the fit for the $|005^u00\rangle - |00000\rangle$ band at $15\,600\text{ cm}^{-1}$. As can be seen from the plot of the residuals in Fig. 2, this fit is quite successful, and there are no signs of perturbations. In contrast, Table III gives the results for the

$|006^u00\rangle - |00000\rangle$ band at $18\,430\text{ cm}^{-1}$. A plot of the residuals for this band (Fig. 3) shows two perturbations, one at $J=8$, the other at $J=20$. The fact that both R and P branch lines which share the same upper level

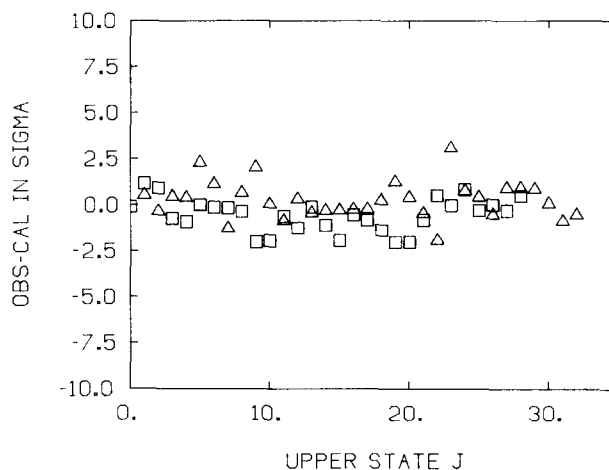


FIG. 2. Residuals, in units of $\sigma = 0.001\text{ cm}^{-1}$, plotted as a function of upper state rotational angular momentum quantum number, for the $^{12}\text{C}_2\text{H}_2$ band at $15\,600\text{ cm}^{-1}$. For a given J , residuals for the P and R branch lines which share the same upper state are plotted. The boxes are residuals for $P(J+1)$; the triangles are for $R(J-1)$.

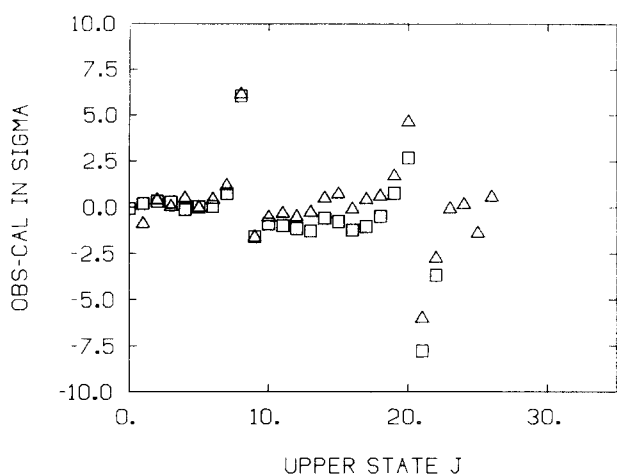


FIG. 3. Residuals in units of $\sigma = 0.004 \text{ cm}^{-1}$, plotted as a function of upper state rotational angular momentum quantum number, for the $^{12}\text{C}_2\text{H}_2$ band at 18430 cm^{-1} . For a given J , residuals for the P and R branch lines which share the same upper state are plotted. The boxes are residuals for $P(J+1)$; the triangles are for $R(J-1)$.

deviate in the same direction, together with the fact that the ground state combination differences are correct, even for the deviant lines, shows the state $|006^u00\rangle$ to be perturbed. For that reason, lines in both the P and R branches near the perturbed levels were omitted from the fit.

Assignments, band origins, rotational constants, distortion constants, and overall standard deviations for the fits calculated from the observed $\Sigma-\Sigma$ bands are listed in Tables IV–VII.²⁷ The wide variation of uncertainties from band to band reflects the degree to which different bands are perturbed, not the uncertainty in determining line positions. In Tables IV, V, and VII, brackets are used to indicate those bands for which an unambiguous assignment of zero order local mode quan-

TABLE IV. Observed $\Sigma-\Sigma$ bands of $^{12}\text{C}_2\text{H}_2$.^{a,b,c}

Upper state assignment	ν_0	$\Delta B \times 10^3$	$-\Delta D \times 10^6$	$\sigma \times 10^3$
$ 113^u00\rangle$	14 968.903(4)	-32.19(4)	0.31(6)	3
$ 005^u00\rangle$	15 600.1643(5)	-32.964(3)	0.025(3)	1
$ 014^u2^00\rangle$	15 690.08(2)	-27.7(6)	-12(2)	34
	15 768.60(2)	-25.2(2)	10.8(5)	18
	15 829.44(2)	-27.9(7)	10(6)	13
$ 104^u00\rangle$	15 948.482(2)	-30.83(3)	0.4	5
	16 500.937(87)	-26.60(90)	6.5(1.7)	149
$ 024^u00\rangle$	16 529.672(23)	-32.94(35)	-5.46(98)	34
	16 541.159(11)	-30.32(21)	-8.04(77)	12
	16 566.082(13)	-35.95(17)	-3.16(39)	20
$ 015^u00\rangle$	17 518.806(5)	-38.02(3)	-0.43(5)	23
$ 006^u00\rangle$	18 430.066(2)	-40.41(2)	0.20(3)	4
	$B_0 = 1.176\ 608(16)$	$D_0 = 1.598(9) \times 10^{-6}$		

^aAll values in cm^{-1} .

^bAll errors are 2σ .

^cAll transitions are $\Sigma-\Sigma$ transitions from the ground state. Ground state constants are taken from Ref. 23.

TABLE V. Observed $\Sigma-\Sigma$ bands of $^{13}\text{C}_2\text{H}_2$.^{a,b,c}

Upper state assignment	ν_0	$\Delta B \times 10^3$	$-\Delta D \times 10^6$	$\sigma \times 10^3$
$ 005^u00\rangle$	15 520.1643(67)	-28.569(43)	2.034(52)	14
	15 531.955(26)	-27.37(60)	3.2(2.3)	35
	15 573.650(38)	-21.89(44)	-4.20(89)	67
	15 726.7237(45)	-23.516(86)	2.11(30)	5
$ 104^u00\rangle$	15 888.5074(68)	-26.543(73)	0.16(14)	11
	15 892.190(18)	-22.60(35)	-0.16(1.1)	26
$ 024^u00\rangle$	16 368.1034(24)	-34.275(23)	-0.322(41)	4
$ 015^u00\rangle$	17 377.197(38)	-32.81(32)	3.05(45)	69
	17 398.776(16)	-32.07(27)	-7.45(83)	25
$ 006^u00\rangle$	18 332.6959(13)	-36.384 2(67)	-2.41(61)	29
	$B_0 = 1.119\ 49(4)$	$D_0 = 1.47(2) \times 10^{-6}$		

^aAll values in cm^{-1} .

^bAll errors are 2σ .

^cAll transitions are $\Sigma-\Sigma$ transitions from the ground state. The ground-state constants are taken from Ref. 25.

tum numbers could not be made, probably due to Fermi resonances.

B. $\Pi-\Sigma$ and $\Pi-\Pi$ bands

The only perpendicular bands seen in any isotopic species were of the type $\Pi-\Sigma$. The Q branches of these bands were fit to the polynomial²²:

$$\nu(J) = \nu_0 - (B^* + D^*) + (B^* - B'' + 2D^*)J(J+1) - (D^* - D'')J^2(J+1)^2, \quad (3)$$

where B^* , D^* are the rotational and distortion constants of the upper component of the l doublet. The P and R branch lines were fit in the same manner as for a $\Sigma-\Sigma$ band, except that the band origin in Eq. (1) is replaced by $\nu_0 - (B^* + D^*)$, where B^* , D^* are the rotational and distortion constants of the lower component of the l doublet.

The $\Pi-\Pi$ bands were fit to the polynomial²²:

$$\begin{aligned} \nu^*(m) = & \nu_0 - \Delta B - \Delta D + [2B'' + \Delta B + 2(2D'' + \Delta D) \\ & \pm 2(2q_0 + \Delta q)]m + [\Delta B - \Delta D \pm 2\Delta q]m^2 \\ & - 2(2D'' + \Delta D)m^3 - \Delta Dm^4. \end{aligned} \quad (4)$$

TABLE VI. Observed $\Sigma-\Sigma$ bands of $^{13}\text{C}^{12}\text{CH}_2$.^{a,b,c}

Upper state assignment	ν_0	$\Delta B \times 10^3$	$-\Delta D \times 10^6$	$\sigma \times 10^3$
$ 50000\rangle$	15 525.5664(30)	-30.668(19)	-0.0685(21)	6
$ 00500\rangle$	15 596.5296(37)	-31.726(29)	-0.248(41)	7
$ 10400\rangle$	15 910.978(9)	-27.24(24)	1.34(57)	26
$ 60000\rangle$	18 338.1573(79)	-36.948(78)	1.08(15)	13
$ 00600\rangle$	18 424.8103(18)	-39.230(20)	0.061(40)	3
	$B_0 = 1.148\ 40(2)$	$D_0 = 1.56(2) \times 10^{-6}$		

^aAll values in cm^{-1} .

^bAll errors are 2σ .

^cAll transitions are $\Sigma-\Sigma$ transitions from the ground state. The ground state constants are taken from Ref. 25.

TABLE VII. Observed $\Sigma-\Sigma$ bands of $^{12}\text{C}_2\text{HD}$.^{a,b,c}

Upper state assignment	ν_0	$\Delta B \times 10^3$	$-\Delta D \times 10^6$	$\sigma \times 10^3$
10400)	15 282.256(33)	-26.81(23)	-2.31(29)	67
	15 315.9439(28)	-22.041(21)	1.618(30)	5
00500)	15 697.086(62)	-28.09(56)	-5.78(89)	121
10500)	18 207.1844(45)	-31.757(45)	-0.614(80)	8
$B_0 = 0.991\,5273(16)$		$D_0 = 1.120(13) \times 10^{-6}$		

^aAll values in cm^{-1} .^bAll errors are 2σ .^cAll transitions are $\Sigma-\Sigma$ transitions from the ground state. The ground state values are taken from Ref. 24.

The l -doubling constant q_0 is defined as $4q_0 = B^+ - B^-$. As before, the “+/-” superscripts refer to the upper and lower components of the l doublet.

The fits for both the $\Pi-\Sigma$ and $\Pi-\Pi$ bands were generally of poorer quality than the $\Sigma-\Sigma$ bands. In the case of $\Pi-\Pi$ bands, this is due mainly to partially resolved l doubling. In both the $\Pi-\Pi$ and $\Pi-\Sigma$ bands, spectral congestion, and blending of lines from overlapping bands was a severe problem. For the $\Sigma-\Pi$ bands, an interesting intensity anomaly was observed, with the R and P branches differing markedly in intensity. The results are given in Tables VIII and IX. In only one case (see Table VIII) is the quality of the data good enough to determine all of the constants. In other cases, even though the standard deviation of the overall fit is quite good, some of the constants remain undetermined due

TABLE X. Comparison of observed $\Sigma-\Sigma$ band origins with origins calculated from anharmonic constants.

Normal mode ^a assignment	Local mode assignment	Observed	Calculated ^b
$^{12}\text{C}_2\text{H}_2$			
(00500)	005 ^u 00	15 600.2	15 824
(20300)	104 ^u 00	15 948.5	15 769
(10500)	006 ^u 00	18 430.1	18 680
$^{13}\text{C}_2\text{H}_2$			
(00500)	005 ^u 00	15 520.2	15 780
(20300)	104 ^u 00	15 888.5	15 683
(10500)	006 ^u 00	18 332.7	18 611

^aFrom Ref. 28.^bFrom the anharmonic constants of Strey and Mills (Ref. 15).

to correlations introduced by the structure of the available data.²⁶

V. VIBRATIONAL ANALYSIS

Table X shows a comparison between the observed band origins and those calculated from the anharmonic constants of Strey and Mills.¹⁵ From these data, it is clear that the usual normal mode, slightly anharmonic expansion cannot be meaningfully extrapolated to this level of excitation. This is in contrast to HCN, where the anharmonic expansion works quite well.¹⁰ For acetylene, the agreement between observed and calculated origins is so bad that correlating the two is difficult for the symmetrical acetylenes, and virtually im-

TABLE VIII. $\Pi-\Pi$ and $\Pi-\Sigma$ bands of $^{12}\text{C}_2\text{H}_2$.^a

Assignment	Type	ν_0	B_0	$D_0 \times 10^6$	$q_0 \times 10^3$	$\Delta B \times 10^3$	$\Delta D \times 10^7$	$\Delta q \times 10^4$	$\sigma \times 10^3$
005 ^u 1 ^l 0)	$\Pi_u - \Pi_g$	15 526.200(16)	1.178 1(15)	ND ^b	ND	-32.53(30)	ND	2.98(74)	14
- 0001 ^l 0)									
005 ^u 01 ^l)	$\Pi_g - \Pi_u$	15 561.8590(72)	1.789 5(30)	2.04(44)	1.163(56)	-33.132(56)	-1.08(42)	-0.215(54)	7
- 00001 ^l)									
005 ^u 01 ^l)	$\Pi_u - \Pi_g$	15 679.793(18)	1.177 3(12)	ND	ND	-32.12(18)	ND	-1.59(32)	13
- 0001 ^l 0)									
005 ^u 1 ^l 0)	$\Pi_u - \Sigma_g$	16 139.0600(30)	1.176 41(24)	ND	ND	-33.872(30)	ND	ND	3
- 00000)									

^aAll values in cm^{-1} .^bND: not determined to a statistically significant level in the fit.TABLE IX. $\Pi-\Pi$ and $\Pi-\Sigma$ bands of $^{13}\text{C}_2\text{H}_2$.^a

Assignment	Type	ν_0	B_0	$D_0 \times 10^6$	$q_0 \times 10^3$	$\Delta B \times 10^3$	$\Delta D \times 10^7$	$\Delta q \times 10^4$	$\sigma \times 10^3$
005 ^u 1 ^l 0)	$\Pi_u - \Sigma_g$	16 052.8811(14)	1.119 577(98)	1.44(27)	ND ^b	-30.630(21)	6.50(66)	ND	2.1
- 00000)									
005 ^u 1 ^l 0)	$\Pi_u - \Pi_g$	15 449.08(7)	1.117 1(24)	ND	4.15(58)	-28.8(5)	ND	ND	144
- 0001 ^l 0)									
006 ^u 1 ^l 0)	$\Pi_u - \Pi_g$	18 243.0596(14)	1.119 72(65)	ND	ND	ND	ND	ND	23
- 0001 ^l 0)									
006 ^u 01 ^l)	$\Pi_g - \Pi_u$	18 289.02(17)	1.045(4)	ND	ND	ND	ND	ND	194
- 00001 ^l)									

^aAll values in cm^{-1} .^bND: not determined to a statistically significant level in the fit.

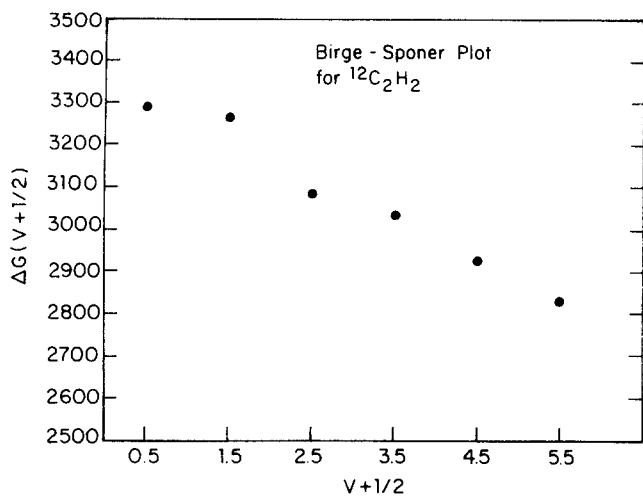


FIG. 4. Birge-Sponer plot for the C-H overtones of $^{12}\text{C}_2\text{H}_2$.

possible for the unsymmetrical species. Furthermore, the anharmonic calculation gives no simple way of predicting relative intensities. If u states having the same number of quanta of C-H stretching excitation are assumed to have similar intensities, then far more bands are predicted than are observed. In contrast, many of the qualitative predictions of a simple local mode theory are borne out in the spectrum of acetylene. For every isotopically substituted acetylene, the strongest bands in the spectrum are $|00v^u00\rangle - |00000\rangle$, where $v = 5$ or 6 . All of the other bands are much weaker, the next strongest being the bands $|1, 0, v-1^u, 0, 0\rangle - |00000\rangle$. The band origins for the pure C-H stretch overtones for ordinary acetylene do indeed fit a linear Birge-Sponer plot (Fig. 4).

The observed Σ states for the different acetylenes are shown graphically in Fig. 5. The isotope shifts for the ^{13}C -substituted acetylenes in the $v = 5$ and 6 manifolds appear to be consistent with the local mode picture. In $^{12}\text{C}^{13}\text{CH}_2$, the states corresponding to five quanta of ^{12}C -H stretch ($|005^u00\rangle$) are only slightly red shifted from the $|005^u00\rangle$ states of $^{12}\text{C}_2\text{H}_2$. The other state, corresponding to five quanta of ^{13}C -H stretch ($|50000\rangle$) is slightly blue shifted from the $|005^u00\rangle$ state of $^{13}\text{C}_2\text{H}_2$. This is precisely what is expected from the independent C-H oscillator model discussed previously. The same pattern is seen for the $v = 6$ manifold, which is not shown in Fig. 5.

However, the isotope shifts for $^{12}\text{C}_2\text{HD}$ are anomalous from this point of view. The $|005^u00\rangle$ level of $^{12}\text{C}_2\text{HD}$ is shifted about 100 cm^{-1} to the blue of the corresponding states in $^{12}\text{C}_2\text{H}_2$ and $^{12}\text{C}^{13}\text{CH}_2$. In the $v = 6$ manifold, which is not shown in Fig. 5, the $|006^u00\rangle$ state of $^{12}\text{C}_2\text{HD}$ is shifted far enough to the blue that it is beyond the range of our dye laser when operating single mode. Low resolution scans indicate that the band origin for this transition is about $18\,564\text{ cm}^{-1}$. Positive identification of this band by combination differences is not possible since we could not observe it at high resolution. The observed shift can be explained by considering the states labeled $|10400\rangle$. For $^{12}\text{C}_2\text{H}_2$ and the ^{13}C sub-

stituted acetylenes, this state corresponds to the excitation of four quanta of CH stretch at one end of the molecule and one quantum of CH stretch at the other end. Due to anharmonicity, the $|10400\rangle$ states are always higher in energy than the $|005^u00\rangle$ states for these molecules. For the ^{13}C substituted acetylenes, the energy of the $|10400\rangle$ state is relatively unaffected by isotopic substitution, so that any interaction between $|10400\rangle$ and $|005^u00\rangle$ is the same in each case. In $^{12}\text{C}_2\text{HD}$, this ordering is reversed since the state $|10400\rangle$ now corresponds to excitation of four quanta of ^{12}C -H stretch and one quantum of ^{12}C -D stretch, which is about 800 cm^{-1} lower in frequency than the ^{12}C -H stretch. Inversion of the ordering of these states gives rise to a blue shift for $|005^u00\rangle$, revealing that there is a substantial interaction energy between $|10400\rangle$ and $|005^u00\rangle$. For $^{12}\text{C}_2\text{HD}$, the band $|10400\rangle$ is almost as intense as the $|005^u00\rangle$ transition. Clearly, the two CH groups in acetylene are not well isolated from each other by the C-C triple bond. This is a breakdown of the local mode model.

Recently, Child and Lawton presented a simple quantitative analysis of local mode behavior in acetylene.²⁸ In their treatment of the problem, a Van Vleck transformation is used to block diagonalize the vibrational Hamiltonian to second order. Each block corresponds to a manifold of states characterized by the total C-H stretching quantum number $v = v_1 + v_3$ and the C-C stretching quantum number v_2 . Within a given manifold, the zero order states are nearly degenerate, being split only by the diagonal anharmonicity. The matrix elements are approximated by their harmonic oscillator values. For evaluation of the second order perturbation

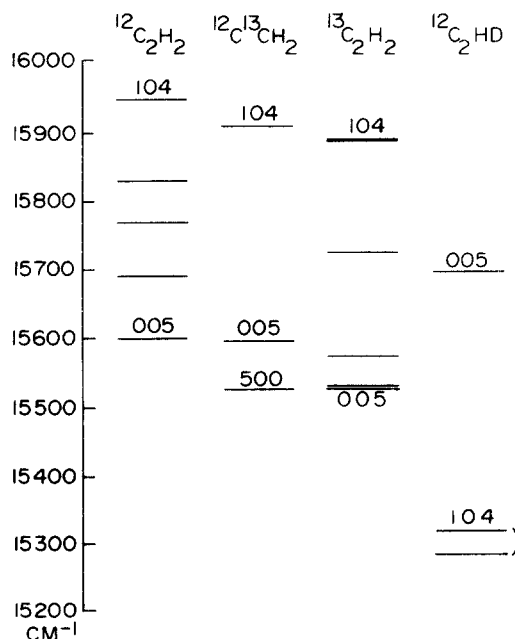


FIG. 5. Energy level diagram for the observed Σ states of $^{12}\text{C}_2\text{H}_2$ between $15\,200$ – $16\,000\text{ cm}^{-1}$. The states are labeled by local mode quantum numbers v_1 , v_2 , and v_3 , as described in the text. The bending quantum numbers v_4 and v_5 , are both zero for the labeled states and have been suppressed for clarity.

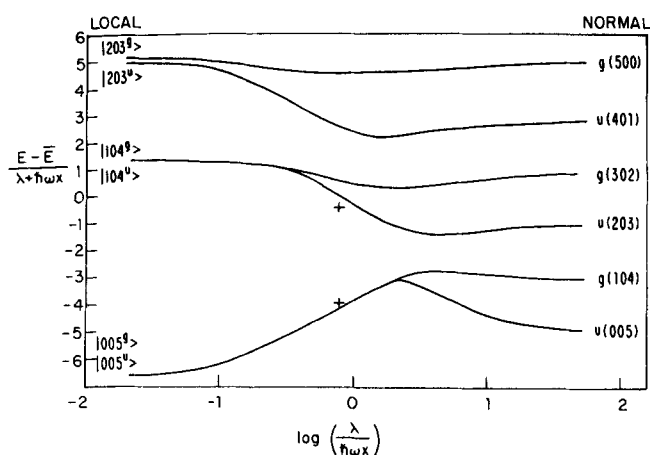


FIG. 6. Correlation diagram. The energy levels of $^{12}\text{C}_2\text{H}_2$ for the $v=5$ manifold are plotted as a function of the log of the ratio of the coupling between the two C-H groups λ to the diagonal C-H anharmonicity ωx . The vertical axis is a reduced energy. E is the average energy of the manifold for each value of $(\lambda/\omega x)$. The two crosses are the observed values. The method used for calculating this graph, originally introduced by Child and Lawton (Ref. 28) is described in detail in the Appendix. On the left, the states are labeled by their local mode quantum numbers v_1 , v_2 , and v_3 . As described in the text, v_1 is one C-H stretch, v_2 is the C-C stretch, and v_3 is the other C-H stretch. The superscripts g and u denote, respectively, the appropriate symmetric and antisymmetric linear combinations of the unsymmetrized local basis functions. On the right, the states are labeled by the normal mode quantum numbers, where v_1 is the symmetric C-H stretch, v_2 is the C-C stretch, and v_3 is the symmetric C-H stretch. The bending quantum numbers have been suppressed for clarity.

corrections, the energy denominators are given harmonic oscillator values. Although these approximations are drastic, they have the advantage that they allow one to express all of the coupling between the two C-H oscillators in terms of a single constant λ . This coupling constant contains both potential and kinetic energy contributions. For acetylene, the kinetic contributions are dominant. These contributions to λ are from indirect kinetic coupling of the two C-H groups through the C-C bond. Child and Lawton have shown that, for a given value of v , the energy level spacings can be either normal modelike or local modelike, depending on the value of $(\lambda/\omega x)$, where ωx is the diagonal CH anharmonicity. We have generalized Child and Lawton's model to permit treatment of unsymmetrical acetylenes. For $^{12}\text{C}_2\text{H}_2$, $^{12}\text{C}^{13}\text{CH}_2$, and $^{13}\text{C}_2\text{H}_2$ this model predicts the isotope shifts in a qualitatively correct manner. However, for $^{12}\text{C}_2\text{HD}$, the model breaks down. Further details on the Child and Lawton model are in the Appendix.

The situation in acetylene is clarified by considering the correlation diagram in Fig. 6, which is similar to that given by Child and Lawton.²⁸ This graph has been recalculated, using the constants listed in the Appendix, to facilitate comparison with our observed band origins for $^{12}\text{C}_2\text{H}_2$, which are included on the plot. The horizontal axis is the logarithm of the ratio of the coupling (λ) to the diagonal CH anharmonicity (ωx). The energy level spacings are normal modelike for $(\lambda/\omega x) \gg 1$, and

local modelike for $(\lambda/\omega x) \ll 1$. Acetylene is seen to be an intermediate case $(\lambda/\omega x) \approx 1$. Thus, either normal mode or local mode basis sets are expected to be very mixed in acetylene. From this point of view, it is not surprising that there is considerable interaction between the local mode basis states $|005\rangle$ and $|104\rangle$. This is also consistent with the observation that, of all the combination bands, $|104\rangle$ is the most intense. Since the basis state $|005\rangle$ carries most of the oscillator strength, the strong interaction between $|104\rangle$ and $|005\rangle$ permits the transition to $|104\rangle$ to steal enough intensity to make it the strongest combination band in the spectrum.

The simple model of Child and Lawton also makes two predictions concerning the states $|005^g00\rangle$ and $|005^u00\rangle$. First, even though far from the local mode limit, Fig. 6 shows that these states should be nearly degenerate. Second, the u state is predicted to be lower in energy. Unfortunately, electric dipole selection rules prevent us from observing the $g-u$ splitting directly in transitions from the ground state. No $\Sigma-\Pi$ bands were seen, so we were unable to determine the $g-u$ splitting for $|005^g00\rangle$ and $|005^u00\rangle$. Relatively few $\Pi-\Pi$ bands

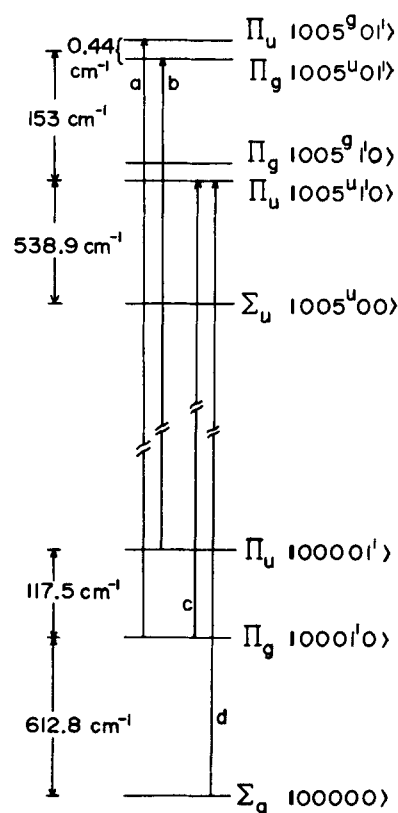


FIG. 7. Energy level diagram showing the observed $\Pi-\Pi$ and $\Sigma-\Pi$ transitions for $^{12}\text{C}_2\text{H}_2$. The $g-u$ splitting of 0.44 cm^{-1} for the two uppermost levels is derived from this level scheme, together with the ground state intervals in Table I, and the transition frequencies, given below (from Table VIII): (a) $15\,679.793(18) \text{ cm}^{-1}$, (b) $15\,561.859(72) \text{ cm}^{-1}$, (c) $15\,526.200(16) \text{ cm}^{-1}$, (d) $16\,139.060(30) \text{ cm}^{-1}$. The state $|005^u00\rangle$ which is at about $15\,600 \text{ cm}^{-1}$, is placed on the graph for reference. Note that the overall symmetry of the states can be decomposed into stretching and bending parts, as follows: $|005^g01^1\rangle \Pi_u = \Sigma_g \times \Pi_u$, $|005^u01^1\rangle \Pi_g = \Sigma_u \times \Pi_u$, $|005^g1^10\rangle \Pi_g = \Sigma_g \times \Pi_g$, $|005^u1^10\rangle \Pi_u = \Sigma_u \times \Pi_g$.

TABLE XI. Comparison of observed Σ - Σ band origins with origins calculated variationally.

Assignment	Observed	Calc. ^a	Assignment	Observed	Calc. ^a
	¹² C ₂ H ₂			¹² C ₂ HD	
113 ^u 00)	14 968.9	14 966.6	10400)	{15 282.3	15 282.3
005 ^u 00)	15 600.2	15 590.9		{15 315.9	15 294.4
	15 690.1		00500)	15 697.0	15 687.8
	15 768.6				
104 ^u 00)	15 829.4		10500)	18 207.2	18 195.9
	15 948.5	15 948.7			
024 ^u 00)	{16 500.9	16 537.1			
	{16 529.7				
	{16 541.2				
	{16 566.1				
015 ^u 00)	17 518.8	17 514.8			
006 ^u 00)	18 430.1	18 410.0			
	¹³ C ₂ H ₂			¹² C ¹³ CH ₂	
005 ^u 00)	15 520.2	15 512.1	50000)	15 525.6	15 514.9
	15 532.0		00500)	15 596.5	15 588.3
	15 573.7		10400)	15 911.0	15 912.2
	15 726.7		60000)	18 338.2	18 318.1
104 ^u 00)	15 888.5	15 888.3	00600)	18 424.8	18 405.2
	15 892.2				
024 ^u 00)	16 368.1	16 362.2			
015 ^u 00)	17 377.2	17 381.4			
	17 398.8				
006 ^u 00)	18 332.7	18 311.0			

^aThe calculated values for ¹²C₂H₂ and ¹³C₂H₂ are from Ref. 30. The calculated values for ¹²C₂HD and ¹²C ¹³CH₂ are from Ref. 31.

were seen, but in the case of ¹²C₂H₂, enough information is available to determine the g - u splitting of the states |005^u01¹) and |005^u01¹). To the extent that bend-stretch interactions can be neglected, this splitting mainly reflects the energy difference between |005^u00) and |005^u00). The energy level scheme for the three observed Π - Π bands and the one Π - Σ band is shown in Fig. 7. The upper states for these transitions are the states constructed from adding one quantum of bending excitation, of either Π_g or Π_u symmetry, to the two states consisting of five quanta of C-H stretching excitation, which have either Σ_g or Σ_u symmetry. The result is a pair of doublets. The spacing between the doublets may be thought of as the difference in frequency of the Π_g or Π_u bends which have been dressed¹² by the excited CH stretching motion. Note that this interval increases in the excited state, even though both of the dressed bending frequencies are lower than that of the bending fundamentals. The assignments in Fig. 7 are consistent with the observed intensity alternation of components in these bands. The g - u splitting for the states |005^u01¹) and |005^u01¹) is observed to be 0.44 cm⁻¹. Child and Lawton's model predicts that the |005^u00) - |005^u00) splitting should be less than 1 cm⁻¹.²⁸ For the excited bending levels observed, the u symmetry local mode combination is lower in energy, in agreement with the prediction of the Child and Lawton model. For comparison, the g - u splitting of the C-H stretching fundamentals (|001^u00) and |001^u00) is about 86 cm⁻¹,¹⁵ and the splitting of the states |001^u01¹) and |001^u01¹) is about 91 cm⁻¹.²⁸ These results are in good agreement with the qualitative predictions of a local mode model. However, the analysis of Child and Lawton shows that

the mere observation that the g - u splitting is small does not permit us to conclude that the states are local in character. The splitting and order of the states |005^u1¹0) and |005^u1¹0) could not be determined since the transition |005^u1¹0) - |00000) was not seen. For the other isotopically substituted acetylenes, there is not enough data for a similar analysis.

Halonen, Carter, and Child have done variational calculations on a linear model of acetylene.^{30,31} The potential they used treats the C-H groups as Morse oscillators, and the C-C group as a harmonic oscillator. Since this potential is for a linear acetylene, it actually represents a mean potential, averaged over the zero point bending oscillations. The Hamiltonian was diagonalized in a local mode, Morse oscillator basis set. The remarkable agreement between observed and calculated energies is shown in Table XI. Note that Halonen's calculation gives very nearly the correct isotope shifts. Although the local mode basis expansion does very well, the states are found to be quite mixed even in this basis, in agreement with the Child and Lawton model. Also, the g - u splitting for the states |005^u00) and |005^u00) is calculated to be only 0.63 cm⁻¹, with the u state lower in energy, again in qualitative agreement with the simpler model.

It is interesting to note, in Table XI, that there are several observed Σ states that do not correlate to any of Halonen's calculated levels. It seems likely that these are Σ states with a significant amount of excited bending character. In one case (see Table IV) we are able to assign the upper state of an observed band to a state with two quanta of bending excitation. This as-

signment is possible because the acetylene band at $15\,690\text{ cm}^{-1}$ continues a progression which was seen in the photographic infrared.¹⁶ This conclusion is supported by the values of the rotational constants and centrifugal distortion constants for these states. In general, α is negative for bending modes and positive for stretching modes.¹³ The value of ΔB for the unassigned states is significantly less negative than for the other assigned states. This is consistent with the idea that these states have a significant amount of bending character. At present, our analysis of these states must remain vague and qualitative. We do not have a theoretical model for bend-stretch coupling in highly vibrationally excited states that would allow us to assign these levels.

VI. PERTURBATION ANALYSIS

As we have already indicated, rotational analysis of the bands of all four acetylenes studied is complicated by rotational perturbations. One particularly striking example of the effect of rotational perturbations in the upper state is found in the Σ - Σ band of $^{12}\text{C}_2\text{H}_2$ at $17\,518\text{ cm}^{-1}$. This band has been assigned as $|015^400\rangle - |00000\rangle$. The upper and lower state combination differences for this band were fit to the usual formulas. The standard deviation for the lower state fit is only 0.0018 cm^{-1} , which is consistent with our experimental error. This lower state fit gives the ground state constants as $B'' = 1.176\,619(29)\text{ cm}^{-1}$ and $D'' = 1.608(29) \times 10^{-6}\text{ cm}^{-1}$, which are consistent with literature values. For the upper state, however, the standard deviation is a factor of 23 larger. Figure 8 shows the residuals for a constrained ground state whole band fit for this band. The two perturbations are very easily seen. It is also clear from this graph that the systematic deviations due to the perturbations are much larger than the statistical errors.

Numerous attempts were made to "deperturb" the observed bands.^{32,33} These attempts were unsuccessful, mainly because every band (except for the $|005^400\rangle - |00000\rangle$ band) is perturbed for at least two values of J . The problem of analyzing these perturbations is made worse by the fact that the avoided crossings which give rise to the perturbations are very sharp. The perturbations generally are observed only as anomalous shifts of the energy levels for particular values of J . In principle, near the avoided crossing, the rotational levels of the perturbing state should borrow oscillator strength by mixing with the observed state. However, in only a handful of cases was the mixing enough to make the perturbing levels observable. In those cases, the crossings were so sharp, and the matrix elements so small, that we only observed one or two new lines. In the presence of multiple perturbations, this did not provide enough information to make nonlinear least-squares fitting procedures practical. Although we cannot perform a complete perturbation analysis on any of the bands, we are able to estimate the magnitudes of perturbation matrix elements for individual rotation-vibration lines from the magnitude of the shifts. In many cases, when the crossings are very sharp and the perturbing states could be identified in both the P and R

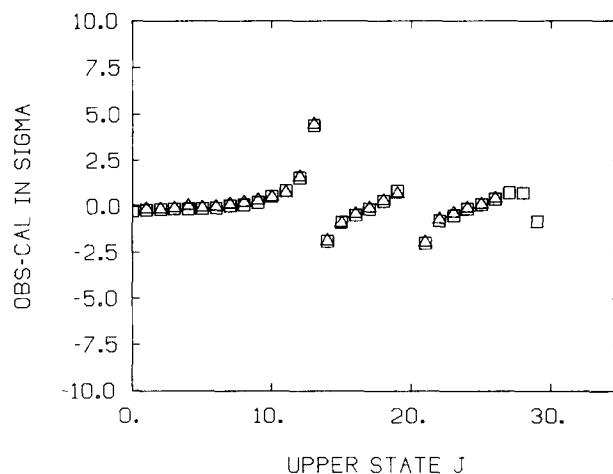


FIG. 8. Residuals, in units of $\sigma = 0.041\text{ cm}^{-1}$, plotted as a function of upper state rotational angular momentum quantum number, for the $^{12}\text{C}_2\text{H}_2$ band at $17\,518\text{ cm}^{-1}$. For a given J , residuals for the P and R branch lines which share the same upper state are plotted. The boxes are residuals for $P(J+1)$; the triangles are for $R(J-1)$.

branches, the matrix elements for individual rotation-vibration states were found to be 0.1 cm^{-1} or less. For example, the two perturbations in the Σ state of $^{12}\text{C}_2\text{H}_2$ at $18\,430\text{ cm}^{-1}$ (see Fig. 3 and Table III) could be analyzed. The perturbation at $J=20$ has a matrix element of 0.04 cm^{-1} , and the perturbation at $J=8$ has a matrix element of 0.077 cm^{-1} . In other cases (see Tables IV-VII) the bands were so congested that it was not possible to identify the perturbing states in both branches. The largest deviations observed from the position predicted by the least-squares fits are on the order of 0.3 cm^{-1} or less for all the bands. Since the zero-order splittings of the states must be on the order of 1 cm^{-1} (based on reasonable estimates for the rotational constants¹⁰), 0.3 cm^{-1} is a good upper bound for the size of the rotational perturbation matrix elements for the bands we observe.

It is interesting to speculate about the number of perturbations seen in acetylene. For $^{12}\text{C}_2\text{H}_2$, simple harmonic counting gives the density of states in the vicinity of $15\,600\text{ cm}^{-1}$ as about $25/\text{cm}^{-1}$. Most of these states are excited bending levels. Since α for the bending modes is negative, while α for the stretches is positive,¹⁴ there should be a large difference in rotational constant between the states we observe and the excited bending levels. Thus, the observed states must be crossed many times by other vibrational levels. Yet, in general, only two or three perturbations per band are seen. It appears that virtually none of the excited bending states are able to couple effectively to the observed stretching states. These observations are consistent with our work on HCN. It seems that a sort of "Franck-Condon" principle applies to the perturbation matrix elements.¹⁰ States differing greatly in degree of bending excitation do not couple very strongly.

In the previous discussion, by perturbation we mean a disruption of the rotational progression. There are also several clear examples in the spectrum of vibra-

tional perturbations, i. e., Fermi resonances. We see several extra bands, whose intensity can only be explained by intensity borrowing from the strong bands. For example, Table IV shows that, in $^{12}\text{C}_2\text{H}_2$ four states are seen in the frequency region where the only level $|024^400\rangle$ is expected. Similarly, in the case of the level $|005^400\rangle$, we see a total of five states which are probably seen only because they steal intensity from the pure local mode state. For this band, however, assignment of the local mode quantum numbers to one band is unambiguous, because the band at $15\,600\text{ cm}^{-1}$ is much more intense than the others. Similar behavior is also seen in $^{13}\text{C}_2\text{H}_2$ (Table V) and in $^{12}\text{C}_2\text{HD}$ (Table VI). The magnitudes of these vibrational matrix elements could not be measured, since we do not have reliable intensity information at present. However, the fact that we observe these levels at all means that the interaction matrix elements must be considerably larger than 0.3 cm^{-1} . In some cases, the weaker bands can be assigned to pure stretching states; in others, as mentioned earlier, they must have some bending excitation. The fact that the number of such resonances is small compared to the total density of states shows that very strong selection rules still apply to the highly excited vibrational states of acetylene.

VII. CONCLUSIONS AND SUMMARY

As is well known and has been demonstrated again here, the overtone spectrum of a molecule as simple as acetylene can be quite complex. Qualitatively, the overtone spectrum of acetylene stands in sharp contrast to the previously studied overtone spectrum of HCN.¹⁰ The vibrational spectrum of HCN in the visible is remarkable for its simplicity. Unlike HCN, nearly every band of acetylene is rotationally perturbed. Also unlike HCN, the usual slightly anharmonic normal mode expansion is inadequate for acetylene. Thus one is led to use a local mode description of the excited states of acetylene.

Based on the usual criteria for local mode behavior, acetylene appears to be an excellent candidate for the local mode description. There is no direct kinetic coupling between the two C-H groups, and the potential coupling is known to be small. The overtones of acetylene give a linear Birge-Sponer plot. The intensities of the observed bands are consistent with the predictions of a simple local mode picture. In the one case where we were able to directly observe the $g-u$ splitting it was found to be small, again in agreement with the expectations of local mode theory.

However, more careful analysis shows drastic departures from local mode behavior. Deuterium substitution gives results that can be understood only in terms of a substantial interaction between the two local C-H oscillators. This is consistent with our observations on deuterated methanes,³⁴ and in marked contrast to the behavior commonly believed to occur in larger systems. The theoretical analysis of Child and Lawton²⁷ shows that acetylene is an intermediate case. Nevertheless, the local mode picture is still a useful device for discussing the overtone spectrum. Even

though the local mode basis provides a better framework for discussing the spectrum than the normal mode basis, the true eigenstates are very mixed in both normal mode and local mode basis sets. However, the energy level spacings for levels with the greatest oscillator strength are local modelike anyway. This result underscores the dangers inherent in trying to draw conclusions about the nature of an effective Hamiltonian by looking at a small subset of its eigenvalues. The fact that the $g-u$ splitting for a pair of states is observed to be small does not permit us to conclude that the states are "local" in character. As can be seen from the correlation diagram in Fig. 6 the $g-u$ splitting for the states $|005^g\rangle$ and $|005^u\rangle$ becomes small far from the local mode limit. At present, we are simply unable to draw any conclusions about the local or "normal" nature of the vibrational overtone states. The work of Brumer *et al.*³⁵ has shown that, classically, it is possible for systems to exhibit both normal modelike and local modelike motion in energetically nearby regions of phase space. This raises the intriguing possibility that some of the observed states are local and others normal in character. This would seem to be consistent with the correlation diagram in Fig. 6. The energy level spacings for some states become local for the same value of $(\lambda/\omega x)$ for which the spacings of other levels remain normal. Such speculations cannot be tested without a means of obtaining vibrational wave functions. Halonen and Child have demonstrated the power of variational calculations for giving accurate term values for these vibrational states.²⁶ Unfortunately, intensities and rotational constants based on their variationally determined wave functions have not yet been calculated. We feel that much information about the vibrational wave functions could be obtained from an analysis of intensities and rotational constants. We have already obtained experimentally a set of precise rotational constants for these overtone states of acetylene, and we plan to make careful measurements of relative intensities in the very near future. It would be interesting to see how the observed values compare to those calculated from variational wave functions.

An interesting question raised by this work concerns the nature of the interaction between bending and stretching degrees of freedom for these highly excited states. Our understanding of these bend-stretch interactions is hampered by our lack of a theoretical model for treating the bending degrees of freedom in highly vibrationally excited acetylene. Such a model is needed for an understanding of the rotational perturbations, as well as for a complete assignment of the observed Σ states in $^{12}\text{C}_2\text{H}_2$ and $^{13}\text{C}_2\text{H}_2$, some of which seem to have excited bending character. If quantum numbers could be assigned to the perturbing states, the amount of information which could be extracted from our data would drastically increase.

Although many rotational perturbations are seen in acetylene while none are observed in HCN, it appears that a Franck-Condon principle applies to the perturbation matrix elements in both cases. In HCN, a few Fermi resonances appear in the spectrum. Similarly, there are several instances in the overtone spectrum of

acetylene in which Fermi resonances mix the oscillator strength of a transition over several states. The dark states that couple in cannot be assigned to stretching states, and so must be assigned to states with bending excitation. Still, the number of interacting levels is much smaller than that expected from a consideration of the total density of states, indicating that strong selection rules govern interactions between these highly vibrationally excited states of acetylene. This is an important observation, since overtone linewidths in larger polyatomic molecules are usually explained in terms of fast intramolecular vibrational relaxation, which is thought to be a consequence of coupling between the initially excited C-H oscillator and a very high density of other molecular states—the “heat bath.” The heat bath is thought to contain a sizeable fraction of the total density of states. The coupling of the initially excited state to this near continuum of levels produces a dissipation process, much as coupling to the radiation field states produces spontaneous emission of excited levels. In the case of acetylene, the large density of states with excited bending degrees of freedom would constitute the heat bath. Since the density of levels is not high enough to appear as a continuum on the time scale of our absorption experiment, dissipation cannot occur. Still, thousands of states are present in the typical bandwidth of 100 cm^{-1} over which the rotational structure of most bands extends. Such heat bath arguments usually ignore the size and physical origin of the couplings, usually leaving them as adjustable parameters.³⁶ Potential energy couplings are difficult to estimate, because potential energy surfaces for polyatomic molecules are not well known. Our results, and the theoretical calculations of Child and Lawton,²⁸ indicate that most of the coupling in acetylene is kinetic in origin. If this is also the case for larger systems, it should be possible to estimate the couplings quite well, since only a knowledge of molecular geometry is needed to calculate the G matrix. Theoretical work by Reinhardt³⁷ indicates that kinetic energy coupling is indeed dominant in the overtone states of benzene. Whether or not such fast intramolecular vibrational relaxation can be accounted for by using physically reasonable matrix elements is a matter of controversy at present. Certainly for acetylene and HCN, a simple density of states approach is inadequate. The density of states which actually couple to the observed levels is much smaller than the total density of states. This is consistent with Reinhardt's work,³⁷ which explains the width of the overtone features of benzene in terms of simple Fermi resonances between the C-H local mode state and a small number of states with one less quantum of C-H stretch and two quanta of the C-H wag normal mode.

We have found that the shifts of the sequence band transitions for the observed stretching states are quite large (about 74 cm^{-1} for the Π_g bend, 39 cm^{-1} for the Π_u bend). Since large molecules, in which large overtone linewidths are observed, have many low frequency vibrations, there are expected to be many intense sequence band transitions built on the main transition spread over a wide frequency range. When this sequence band congestion is combined with rotational congestion and the

presence of even a small number of Fermi resonances, the broad features commonly observed in overtone spectra are easily rationalized. Consequently, the width of overtone transitions in many larger polyatomic molecules can be explained without invoking intramolecular vibrational relaxation. Therefore the linewidth cannot be used directly to establish the strength of coupling to the heat bath. Nearly all experiments performed to date on overtones of large polyatomic molecules have been linear absorption experiments on static gas samples. Such experiments are inherently incapable of distinguishing between a true homogeneous spectral feature and spectral congestion.

The lone exception to date is the experiment of West *et al.*³⁸ In this experiment, direct overtone spectra of tetramethyldioxetane, cooled in a supersonic jet, were taken in the region of five quanta of C-H stretching excitation. The width of the absorption features were found to be the same in both the bulk gas and in the jet. Although very suggestive, this experiment suffers from several ambiguities, the most severe of which is the lack of any direct measure of the vibrational temperature of the jet-cooled tetramethyldioxetane. It is well known that vibrational degrees of freedom are often poorly cooled in jet expansions under conditions which give very low rotational temperatures.³⁹ In addition, there is indeed a qualitative difference between the spectra taken in a jet and those taken in the gas phase—the relative intensities of two features in the spectrum changes considerably. Finally, the width of the laser used in this experiment was too large to resolve rotational structure in a molecule this large, and the signal to noise was too low to distinguish partially resolved structure from noise. We make these points simply to indicate that further work on this problem is needed to clarify the interpretation of these spectra.

The success of the quasicontinuum model of infrared multiphoton absorption has also been used to support the interpretation of overtone linewidths as due to fast intramolecular vibrational relaxation. Indeed, the quasicontinuum model would seem to imply that the overtone states must relax rapidly. However, recent work on small polyatomic molecules has shown that these can also undergo infrared multiphoton absorption. Here the density of levels is so small that, even if all the levels are optically coupled, it is difficult to understand how significant pumping can occur. For example, HN_3 has been observed to absorb about 19 CO_2 laser photons under collision-free conditions.⁴⁰ However, the N-H stretching overtone spectra of HN_3 in the vicinity of five and six quanta of N-H stretching excitation show Doppler-limited features.³⁴ Also, these spectra indicate that the amount of intramolecular coupling, as evidenced by rotational and Fermi resonances, is small. This is especially surprising, since the $v=6$ states of HN_3 are just above, or possibly just below, the dissociation limit of HN_3 .³⁴ This demonstrates that the existence of infrared multiphoton absorption does not imply that the overtone states are strongly mixed with the other states.

Intramolecular vibrational relaxation has also been explained as a quantum mechanical analog of classical

chaotic motion.⁴¹ For comparison, we have calculated classical trajectories for linear acetylene, using a coupled Morse oscillator potential. Our results, as well as those of Noid, who has done trajectory calculations on the potential of Halonen, Carter, and Child indicate that the classical motion is quasiperiodic for total energies below 30 000 cm⁻¹.⁴² These calculations ignore the bending degrees of freedom; however, our work with HCN seems to indicate that neglect of bending does not affect the energy at which trajectories become chaotic.¹⁰ Subsequent work⁴³ indicates that the energy at which trajectories become chaotic depends critically on the potential. At present, there is no polyatomic molecule for which the potential is known well enough to determine the energy at which the molecular dynamics become chaotic. Since the trajectories for these potentials of acetylene in the energy region for which we have data are quasiperiodic, it would be interesting to see the results of semiclassical quantization on the potential of Halonen *et al.*²⁶ This might shed some light on the character of the vibrational states we observe.

ACKNOWLEDGMENTS

We would like to thank Dr. Lauri Halonen and Dr. Mark Child for making the results of their variational calculations on acetylene available to us prior to publication, and for useful discussions on the nature of the local mode model. We would also like to acknowledge Pete Haaland for synthesizing ¹²C₂HD for us.

APPENDIX

The model of Child and Lawton, as derived in Ref. 28, is directly applicable only to symmetrical acetylenes. In this appendix, we describe a generalization of their model which allows treatment of the unsymmetrical ¹²C¹³CH₂.

In this model of the vibrations of a linear acetylene, the displacement coordinates for the two C-H oscillators are denoted r_1 and r_3 . The displacement coordinate for the C-C bond is denoted by r_2 . The mass of the i th atom is m_i , where m_1 and m_4 are the masses of the hydrogen atoms, and m_2 and m_3 refer to the carbon atoms. Let $\mu_i = (1/m_i)$. The G matrix is then

$$G = \begin{bmatrix} \mu_1 + \mu_2 & -\mu_2 & 0 \\ -\mu_2 & \mu_2 + \mu_3 & -\mu_3 \\ 0 & -\mu_3 & \mu_3 + \mu_4 \end{bmatrix}.$$

The zero order Hamiltonian is

$$H^0 = \sum_{i=1}^3 G_{ii} P_i^2 + V_1(r_1) + V_3(r_3) + kr_2^2.$$

The potentials $V_i(r_i)$ are taken to be Morse potentials so that the eigenvalues of H^0 are

$$E^0(v_1, v_2, v_3) = (v_1 + \frac{1}{2})\hbar\omega_1 - (v_1 + \frac{1}{2})^2\hbar\omega x_1 + (v_2 + \frac{1}{2})\hbar\omega_2 + (v_3 + \frac{1}{2})\hbar\omega_3 - (v_3 + \frac{1}{2})^2\hbar\omega x_3.$$

The perturbation Hamiltonian is

$$H' = k_{13}r_1r_3 + k_{12}r_2(r_1 + r_3) - p_2(\mu_1p_1 + \mu_3p_3).$$

Matrix elements are approximated by their harmonic

TABLE XII. Matrix elements of the perturbation Hamiltonian H' .

Δn_1	Δn_2	Δn_3	$\langle n_1 + \Delta n_1, n_2 + \Delta n_2, n_3 + \Delta n_3 H' n_1, n_2, n_3 \rangle$
1	0	1	$\beta [(n_1 + 1)(n_3 + 1)]^{1/2}$
-1	0	-1	$\beta [n_1 n_3]^{1/2}$
1	0	-1	$\beta [(n_1 + 1)n_3]^{1/2}$
-1	0	1	$\beta [n_1(n_3 + 1)]^{1/2}$
1	1	0	$(\delta + \eta)[(n_1 + 1)(n_2 + 1)]^{1/2}$
-1	-1	0	$(\delta + \eta)[n_1 n_3]^{1/2}$
1	-1	0	$(\eta - \delta)[(n_1 + 1)n_2]^{1/2}$
-1	1	0	$(\eta - \delta)[n_1(n_2 + 1)]^{1/2}$
0	1	1	$(\gamma + \xi)[(n_2 + 1)(n_3 + 1)]^{1/2}$
0	-1	-1	$(\gamma + \xi)[n_2 n_3]^{1/2}$
0	1	-1	$(\xi - \gamma)[(n_2 + 1)n_3]^{1/2}$
0	-1	1	$(\xi - \gamma)[n_2(n_3 + 1)]^{1/2}$

$$\beta = \frac{\hbar}{2} \left[\frac{(\mu_1 + \mu_2)(\mu_3 + \mu_4)}{k^2} \right]^{1/4}$$

$$\delta = \frac{\hbar}{2} \mu_2 \left[\frac{k k_2}{(\mu_1 + \mu_2)(\mu_2 + \mu_3)} \right]^{1/4}$$

$$\gamma = \frac{\hbar}{2} \mu_3 \left[\frac{k k_2}{(\mu_2 + \mu_3)(\mu_3 + \mu_4)} \right]^{1/4}$$

$$\eta = \frac{\hbar}{2} k_{12} \left[\frac{k k_2}{(\mu_1 + \mu_2)(\mu_2 + \mu_3)} \right]^{-1/4}$$

$$\xi = \frac{\hbar}{2} k_{12} \left[\frac{k k_2}{(\mu_2 + \mu_3)(\mu_3 + \mu_4)} \right]^{-1/4}$$

oscillator values

$$p_i |v_i\rangle = -i \left(\frac{\hbar}{2} \right)^{1/2} (\mu k)^{1/4} [-(v_i + 1)^{1/2} |v_i + 1\rangle + v_i^{1/2} |v_i - 1\rangle],$$

$$r_i |v_i\rangle = \left(\frac{\hbar}{2} \right)^{1/2} (\mu k)^{-1/4} [(v_i + 1)^{1/2} |v_i + 1\rangle + v_i^{1/2} |v_i - 1\rangle],$$

where k is the C-H stretching force constant. The derivation follows that of Ref. 28 very closely and will not be repeated here. The nonzero matrix elements of H' for the unsymmetrical acetylenes are given in Table XII, in terms of the coupling constants. Child and Lawton express the coupling in terms of three constants β , α_c , and β_c . Our constant β is identical to theirs, and scales the direct potential coupling between the two C-H oscillators. For symmetrical acetylenes, our constants collapse to $\alpha_c = \gamma = \delta$ and $\beta_c = \eta = \xi$. The constants γ and δ are a measure of the strength of the kinetic coupling between the C-H and C-C groups, while η and ξ are a measure of the potential coupling between the C-H and C-C groups. For symmetrical acetylenes, Child and Lawton define the overall coupling constant λ as

$$\lambda = -\alpha + \beta + \frac{(\alpha_c - \beta_c)^2}{\hbar(\omega_1 - \omega_2)} - \frac{(\alpha_c + \beta_c)^2}{\hbar(\omega_1 + \omega_2)}.$$

To simplify the problem so that one need only consider an effective Hamiltonian for a single manifold (defined by $v = v_1 + v_3$ and v_2), interactions with other vibrational manifolds are introduced through second order perturbation theory (i.e., a Van Vleck transformation). Child and Lawton calculate the perturbation corrections assuming that the energy denominators can be approximated by their harmonic oscillator values. With the matrix elements and constants in Table XII, the per-

turbation corrections can be worked out easily, so the formulas need not be listed here.

Table XIII gives the constants used in our calculation. Note that the kinetic energy coupling constants are much larger than the potential energy couplings. The results of our calculation for the $v_1 + v_3 = 5$, $v_2 = 0$ manifolds of $^{12}\text{C}_2\text{H}_2$, $^{13}\text{C}_2\text{H}_2$, and $^{12}\text{C}^{13}\text{CH}_2$ are given in Table XIV.

Note that the isotope shifts are in reasonably good agreement with experiment. $^{12}\text{C}_2\text{HD}$ cannot be treated easily by this model, because the C-H and C-D stretching frequencies are so different that the idea of a nearly degenerate manifold of states defined by $v_1 + v_3$ is no longer meaningful. An attempt to apply the model to $^{12}\text{C}_2\text{HD}$ failed due to accidental degeneracies caused by the fact that the $^{12}\text{C}-^{12}\text{C}$ and $^{12}\text{C}-\text{D}$ stretching frequencies are nearly equal. Our results for $^{12}\text{C}_2\text{H}_2$ are different from those of Child and Lawton, and are in better agreement with experiment for the $v = 5$ states (Table XIV). The constants used in our calculation were obtained differently from those used in Child and Lawton's analysis. We used the potential constants from the acetylene force field calculated by Strey and Mills¹⁵ to explicitly calculate ω' and λ . Child and Lawton obtained values for these two constants from a consideration of the observed level splittings. It should be noted that the last term in Child and Lawton's expression for ω' [their Eq. (25)] has the wrong sign. Also, a term is missing in Eq. (22), although it reappears in Eq. (25).

A calculation was also done in which the energy denominators in the perturbation theory corrections were given their Morse oscillator values. The results were generally worse. The $g-u$ splittings increased, and the isotope shifts became much larger. Inclusion of the anharmonicity in the calculation of the energy denominators changes some of the off-diagonal matrix elements by as much as 50%. In the harmonic approximation, there is near cancellation of perturbation corrections, because the energy levels are equally spaced. If the restriction to harmonic selection rules is removed, then the model breaks down. Since the agreement

TABLE XIII. Constants used in the calculation of isotope shifts for acetylene.

Constant ^{a,b}	$^{12}\text{C}_2\text{H}_2$	$^{12}\text{C}^{13}\text{CH}_2$	$^{13}\text{C}_2\text{H}_2$
k ($\text{aJ}\text{\AA}^{-2}$)	6.370	6.370	6.370
k_2 ($\text{aJ}\text{\AA}^{-2}$)	16.341	16.341	16.341
k_{12} ($\text{aJ}\text{\AA}^{-2}$)	-0.095	-0.095	-0.095
k_{13} ($\text{aJ}\text{\AA}^{-2}$)	-0.019	-0.019	-0.019
ωx (cm^{-1})	58.4	58.4, 58.7	58.7
β (cm^{-1})	-5.104	-5.096	-5.089
δ (cm^{-1})	265.99	268.6	250.9
γ (cm^{-1})	265.99	248.3	250.9
η (cm^{-1})	-12.63	-12.51	-12.36
ξ (cm^{-1})	-12.63	-12.48	-12.36
λ (cm^{-1})	44.4	...	36.0
$\underline{\lambda}$ (cm^{-1})	0.76	...	0.61
ωx			

^aConstants above the line are taken from Ref. 15.

^bConstants below the line are derived from those above; see Table XII.

TABLE XIV. Results of model calculation of isotope shifts of acetylene.

State	$^{12}\text{C}_2\text{H}_2$	$^{13}\text{C}_2\text{H}_2$	State	$^{12}\text{C}^{13}\text{CH}_2$
005 ^u	15 568.1	15 474.6	005	15 566.7
005 ^f	15 568.5	15 474.8	500	15 476.0

worsens when the model is improved, it would appear that the success of this model is to some extent fortuitous. This should not be surprising; the approximations invoked to reduce the coupling to a single parameter (λ) are very drastic. However, even after improvement, the model still gives qualitatively correct behavior. Thus it provides an indispensable physical picture of the interactions between the local mode basis states in acetylene.

- ¹G. Herzberg, *Infrared and Raman Spectra* (Van Nostrand, New York, 1945).
- ²Y. H. Pao, *Optoacoustic Spectroscopy and Detection* (Academic, New York, 1977).
- ³R. L. Swofford, M. E. Long, and A. C. Albrecht, *J. Chem. Phys.* **65**, 179 (1976).
- ⁴K. V. Reddy, D. F. Heller, and M. J. Berry, *J. Chem. Phys.* **76**, 2814 (1982).
- ⁵B. R. Henry, *Acc. Chem. Res.* **10**, 207 (1976).
- ⁶R. G. Bray and M. J. Berry, *J. Chem. Phys.* **71**, 4909 (1979).
- ⁷D. F. Heller and S. Mukamel, *J. Chem. Phys.* **70**, 463 (1979).
- ⁸J. S. Wong and C. B. Moore, paper presented at the Photoacoustic Spectroscopy Conference, June 1981, Berkeley.
- ⁹J. Pliva and A. S. Pine, *J. Chem. Phys.* **93**, 209 (1982).
- ¹⁰K. K. Lehmann, G. J. Scherer, and W. Klemperer, *J. Chem. Phys.* **77**, 2853 (1982).
- ¹¹R. Mecke and R. Ziegler, *Z. Phys.* **101**, 405 (1936).
- ¹²M. L. Sage and J. Jortner, in *Photoselective Chemistry*, edited by J. Jortner, R. D. Levine, and S. A. Rice (Academic, New York, 1981), Part I, pp. 293-322.
- ¹³I. Abram, A. Martino, and R. Frey, *J. Chem. Phys.* **76**, 5727 (1982).
- ¹⁴E. B. Wilson, J. C. Decius, and P. C. Cross, *Molecular Vibrations* (McGraw-Hill, New York, 1955).
- ¹⁵G. Strey and I. M. Mills, *J. Mol. Spectrosc.* **59**, 103 (1976).
- ¹⁶G. Herzberg, *Infrared and Raman Spectra* (Van Nostrand, New York, 1945), pp. 288-293.
- ¹⁷E. Kritchman, S. Shtrikman, and M. Slatkine, *J. Opt. Soc. Am.* **68**, 1257 (1978); S. Shtrikman and M. Slatkine, *Appl. Phys. Lett.* **31**, 830 (1977).
- ¹⁸S. Gerstenkorn, and P. Luc, *Atlas Du Spectre D'Absorption De La Molecule D'Iode*, CNRS (1978). S. Gerstenkorn and P. Luc, *Rev. Phys. Appl.* **14**, 791 (1979). All reported frequencies in the present work have been corrected by -0.0056 cm^{-1} .
- ¹⁹J. S. Wong, *J. Mol. Spectrosc.* **82**, 449 (1980).
- ²⁰L. Lompa-Krzymien and L. C. Leitch, *Synthesis* **1976**, 124 (1976).
- ²¹F. W. Loomis and R. W. Wood, *Phys. Rev.* **32**, 223 (1928).
- ²²H. C. Allen and P. C. Cross, *Molecular Vib-Rotors* (Wiley, New York, 1963).
- ²³A. Baldacci, S. Gershetti, S. C. Hurlock, and K. Narahari Rao, *J. Mol. Spectrosc.* **59**, 116 (1976).
- ²⁴J. Pliva, *J. Mol. Spectrosc.* **44**, 145 (1972).
- ²⁵W. S. Lafferty and R. J. Thibault, *J. Mol. Spectrosc.* **14**, 79 (1964).
- ²⁶D. L. Albritton, A. L. Schmeltekopf, and R. N. Zare, in

- Molecular Spectroscopy: Modern Research*, edited by K. Narahari Rao (Academic, New York, 1976), Vol. II, pp. 1-68.
- ²⁷A complete listing of the assigned lines for each isotopically substituted acetylene will be published in the Ph.D. thesis of G. Scherer. The list may be obtained by writing the authors.
- ²⁸M. S. Child and R. T. Lawton, *Faraday Discuss. Chem. Soc.* **71**, 273 (1981).
- ²⁹J. F. Scott and K. Narahari Rao, *J. Mol. Spectrosc.* **201**, 438 (1966); A. Baldacci, S. Gershetti, and K. Narahari Rao, *ibid.* **48**, 600 (1973).
- ³⁰L. Halonen, M. S. Child, and S. Carter, *Mol. Phys.* **47**, 1097 (1982).
- ³¹L. Halonen (private communication).
- ³²G. W. Funke, *Z. Phys.* **104**, 169 (1936).
- ³³J. W. C. Johns and W. B. Olson, *J. Mol. Spectrosc.* **39**, 479 (1971).
- ³⁴G. Scherer, K. Lehmann, and W. Klemperer (unpublished results).
- ³⁵C. Jaffe and P. Brumer, *J. Chem. Phys.* **11**, 5646 (1980).
- ³⁶M. Sage and J. Jortner, *Chem. Phys. Lett.* **62**, 451 (1979).
- ³⁷E. L. Sibert III, W. P. Reinhardt, and J. T. Hynes, *J. Chem. Phys.* (submitted).
- ³⁸G. A. West, R. P. Mariella, Jr., J. A. Pete, W. B. Hammond, and D. F. Heller, *J. Chem. Phys.* **75**, 2006 (1981).
- ³⁹R. E. Smalley, L. Wharton, and D. H. Levy, *J. Chem. Phys.* **63**, 4977 (1975).
- ⁴⁰T. Simpson, E. Mazur, I. Burak, N. Bloembergen, and K. Lehmann (unpublished results).
- ⁴¹P. Brumer, in *Photoselective Chemistry*, edited by J. Jortner, R. D. Levine, and S. A. Rice (Academic, New York, 1981), Part I, p. 201.
- ⁴²D. W. Noid (private communication).
- ⁴³K. K. Lehmann, G. J. Scherer, and W. Klemperer, *J. Chem. Phys.* **78**, 608 (1983).